MRI ductography of contrast agent distribution and leakage in normal mouse mammary ducts and ducts with *in situ* cancer

Erica Markiewicz[a], **Xiaobing Fan**[a], **Devkumar Mustafi**[a], **Marta Zamora**[a], **Suzanne D. Conzen**[b], and **Gregory S. Karczmar**[a,*]

[a]Department of Radiology, The University of Chicago, Chicago, IL, USA

[b]Medicine, Hematology/Oncology, The University of Chicago, Chicago, IL, USA

Abstract

High resolution 3D MRI was used to study contrast agent distribution and leakage in normal mouse mammary glands and glands containing *in situ* cancer after intra-ductal injection. Five female FVB/N mice (~19 weeks old) with no detectable mammary cancer and eight C3(1) SV40 Tag virgin female mice (~15 weeks old) with extensive *in situ* cancer were studied. A 34G, 45° tip Hamilton needle with a 25uL Hamilton syringe was inserted into the tip of the nipple and approximately 15uL of a Gadodiamide was injected slowly over one minute into the nipple and throughout the duct on one side of the inguinal gland. Following injection, the mouse was placed in a 9.4 T MRI scanner, and a series of high resolution 3D T1-weighted images was acquired with a temporal resolution of 9.1 minutes to follow contrast agent leakage from the ducts. The first image was acquired at about 12 minutes after injection. Ductal enhancement regions detected in images acquired between 12 and 21 minutes after contrast injection was five times smaller in SV40 mouse mammary ducts (p < 0.001) than in non-cancerous FVB/N mouse mammary ducts, perhaps due to rapid washout of contrast agent from the SV40 ducts. The contrast agent washout rate measured between 12 minutes and 90 minutes after injection was ~20% faster (p < 0.004) in SV40 mammary ducts than in FVB/N mammary ducts. These results may be due to higher permeability of the SV40 ducts, likely due to the presence of *in situ* cancers. Therefore, increased permeability of ducts may indicate early stage breast cancers.

Keywords

MRI ductography; mouse mammary gland; 3D MRI; ductal injection; contrast agent

1. Introduction

Ductal carcinoma *in situ* (DCIS) is an early form of breast cancer that grows in mammary ductal lumens. The frequency of DCIS diagnoses has increased significantly since

*Address correspondence to: Gregory Karczmar, Ph.D., Professor, Department of Radiology, MC2026, University of Chicago, 5841 S. Maryland Ave., Chicago, IL, USA 60637, Phone: 773-702-0214, gskarczm@uchicago.edu.

mammography screening came into routine clinical practice, and DCIS now accounts for up to 25% of all newly diagnosed breast cancers in the United States [1]. It is generally accepted that while some forms of DCIS are life-threatening, a large percentage of DCIS does not progress to the invasive stage and is not clinically significant [2]. There are currently no generally accepted methods for reliably distinguishing indolent from aggressive DCIS, and currently in the U.S. most DCIS is surgically removed.

Mammography is the most commonly used breast cancer screening method, but there are limitations including the relatively high false-positive and false-negative rates, limited sensitivity to DCIS in women with dense breasts, and exposure to radiation [3]. MRI shows promise for detecting DCIS and differentiating between indolent and aggressive DCIS. However, while the sensitivity and specificity of current MRI methods for invasive breast cancer is high, sensitivity and specificity for DCIS is modest [4]. Thus, there is a critical need for new approaches to detecting DCIS and for new image-based markers for DCIS. To address this challenge, we are using MRI ductography of a murine model of breast cancer to improve the understanding of the biology and natural history of DCIS, and to identify new methods and image-based markers that can be used to detect and evaluate DCIS.

Ductography is used clinically to detect small breast cancers [5, 6]. A tiny blunt-tipped needle is used to inject 0.2 – 0.4 mL of contrast agent in order to study the inside of a duct. The outlines of a duct's pathway can be evaluated to determine whether a duct is dilated. Slawson and Johnson, and Ishikawa et al. [7, 8] demonstrated that dynamic contrast enhanced MR ductography is useful for detecting and evaluating intraductal breast cancers. Intra-ductal injections are also performed in mouse mammary glands to inject cancer cells that produce *in situ* cancers [9], and for localized drug delivery [10]. Recent research on FVB/N mice in this laboratory demonstrated that high resolution 3D MRI ductography has the potential to provide unique and important information about architecture, anatomy, and permeability of mammary glands [11].

The present study builds on previous work by using MRI ductography to evaluate contrast agent distribution and leakage from ducts in both FVB/N and SV40 Tag-expressing mice. We tested the hypothesis that contrast agent leakage is faster in ducts with *in situ* cancer than in non-cancerous ducts. The C3(1) SV40 large T antigen (Tag) transgenic mouse is a widely used model of breast cancer [12]. This mouse model targets the expression of large T-antigen to the female mammary gland via the C3(1) promoter. Female SV40 Tag mice develop mammary cancer that resembles human ductal breast carcinoma, including progression through atypical ductal hyperplasia (~8 weeks), DCIS (~12 weeks) and invasive ductal carcinoma (IDC) (~16 weeks) [13, 14]. Prior studies demonstrated that a wide range of growth rates were observed in SV40 transgenic mammary cancers [15]. Most cancers transitioned to the invasive phenotype at approximately 17 weeks of age. Therefore, performing MRI ductography on SV40 mice before 17 weeks of age may provide important information regarding the early development of *in situ* cancers.

2. Materials and methods

2.1 Animals and Ductal injections

All procedures were carried out in accordance with our Institution's Animal Care and Use Committee approval. A total of five female FVB/N virgin mice (average age ~19 weeks, average weight ~24 g) and eight female C3(1) SV40 large T antigen (Tag) transgenic virgin mice (average age ~15 weeks, average weight ~19 g) were used in this study. The FVB/N mice were purchased from Charles River Laboratories, Inc. and SV40 mice were produced in Dr. Conzen's laboratory.

Mice were anesthetized in a rodent anesthesia box under 3–5% isoflurane and 2 L/min O_2, then transferred to a nose-cone and kept anesthetized at 1.5–2.5% isoflurane. The fur was shaved from the skin around the body and hind limbs. The body was wiped with alcohol to remove loose fur and to help visualize the nipples. A 34G, 45° tip Hamilton needle attached to a 25uL Hamilton syringe was then inserted into the tip of the nipple near the inguinal gland. Approximately 15uL of a Gadodiamide solution (0.8 mM Gd chelate, Omniscan GE Healthcare Novation Princeton, NJ, USA) was slowly injected into the nipple over one minute to fill the ducts. We injected only the inguinal mammary gland on one side of each mouse with contrast agent so that the inguinal gland on the opposite side of the mouse could serve as a control. The right mammary gland was picked as the injection site in most mice. However, for the SV40 mice, the left mammary gland was selected for injection when there was a relatively larger tumor, which would prohibit flow of the contrast agent, on the right side. As a result, all FVB/N mice were injected on the right side, four SV40 mice were injected on right side, and four were injected on the left side. A cancer was classified as *in situ* when its size was between 150 – 400 microns, and classified as invasive if its size was >400 microns in largest diameter, based on previous work from this group that correlated cancers on MRI with histology [16].

2.2 MRI experiments

MR imaging was performed on a 9.4 Tesla small animal scanner (Bruker, Billerica, MA, USA) with 11.6 cm inner diameter, actively shielded gradient coil (maximum constant gradient strength for all axes: 230 mT/m), and a 30 mm diameter quad RF coil (RAPID MR International, Columbus, Ohio, USA). Mice were monitored for respiration, temperature, and heart rate using an MRI-compatible physiological monitoring system (SA Instruments, Stoneybrook, NY, USA). Mice were kept at normal body temperature by using warm air blown through the bore of the magnet.

Prior to contrast agent injection, axial multi-slice rapid acquisition refocused echo (RARE) T2-weighted (T2W) images with fat suppression ($TR/TE_{effective}$ = 4000/20.3 ms, FOV = 25.6×19.2 mm, matrix size = 256×192, slice thickness = 0.5 mm, number of slice = 41, RARE factor = 4, NEX = 2) were acquired to provide anatomic information. Then, 3D T1-weighted (T1W) fast low angle shot (FLASH) images (TR/TE = 22.2/4.4 ms, flip angle = 15°, FOV = 25.6×19.2×38.4 mm, matrix size = 256×192×192, partial Fourier factor = 1.5, NEX = 1) with fat suppression were acquired. The mouse was afterwards transferred to a lab bench for the ductal injection.

Following injection, the mouse was immediately secured on an animal holder and inserted into the coil. The first image acquisition began approximately 12 min after the ductal injection. The 3D T1W images with the same parameters as above were acquired repeatedly for about 90 min to follow the contrast agent washout with temporal resolution of 9.1 min. At the end of experiments, axial multi-slice RARE T2W images with the same parameters as above and with fat suppression were acquired to provide anatomic information.

2.3 Data analysis

The data were processed and analyzed quantitatively using software written in IDL (Exelis VIS, Inc., Boulder, CO, USA). To assist with visualizing the ductal architecture, Amira 3D visualization and analysis software (FEI Visualization Sciences Group, Burlington, MA, USA) was used for volume rendering.

The 1st T1W scan acquired between ~12 minutes and 21 minutes after contrast agent injection was used to identify voxels with significant contrast agent uptake. From axial T1W images (with the aid of T2W images), the slice containing the injection site was identified first. Then, the average reference signal intensity (S_{ref}) was calculated over a manually traced region-of-interest (ROI) on the control side of the mammary gland (the side of the mouse that was not injected with contrast agent), excluding the lymph node. Similarly, an ROI was traced around the mammary gland on the side of the mouse that received a contrast media injection. On the contrast-enhanced side of the mouse, only the voxels in the mammary gland with signal intensity greater than four to six times S_{ref} were classified as 'significantly enhanced'. This threshold value was empirically determined to include all enhanced voxels in the ducts and minimize the background signal. The total volume of tissue with significant enhancement ($V_{enhanced}$) was calculated from the sum of all significantly enhancing voxels.

Once those voxels with significant contrast agent uptake were identified, the plot of signal intensity vs. time ($S(t)$) for each voxel was fitted with the following equation to extract the decay constant (λ):

$$S(t) = A \cdot \exp(-\lambda t) + B, \quad (1)$$

where A+B is the maximum signal intensity at time zero and B is the estimated baseline signal intensity at an 'infinite' time after injection.

In addition to the mammary gland, we also observed the signal enhancement post-contrast agent injection in blood vessels. To measure contrast agent washout in the lower aorta following intra-ductal injection, an ROI was manually defined to cover the largest portion of aorta in a coronal slice from the first T1W scan. Then, an empirically determined threshold signal intensity of 10 times S_{ref} was used to identify pixels with significant contrast agent uptake in the aorta within that ROI. The average signal intensity over the aorta was calculated for pixels with signal above the threshold value. Subsequently, the average signal intensity vs. time curve ($S_{aorta}(t)$) was fitted with Eq. 1 to extract the decay constant.

The non-parametric Mann-Whitney U-Test was performed to determine whether there was a statistically significant difference between FVB/N mice and SV40 mice for calculated parameters. A p-value of less than 0.05 was considered significant.

3. Results

Based on size criteria defined for *in situ* and invasive cancers as previously published [16], we identified a total of 31 *in situ* cancers and 10 invasive tumors (Table 1) in the inguinal mammary glands of eight SV40 mice by examining all MRI slices through the glands. No cancers were found in the FVB/N mice. Figure 1 shows an axial MRI slice for an SV40 mouse: (a) pre-contrast agent injection T2W image, (b) a corresponding pre-contrast agent injection T1W image, (c) ~90 min post-contrast agent injection T2W image, and (d) the corresponding first T1W post-contrast agent injection image, acquired between 12 minutes and 21 minutes after injection. The mammary gland injected with contrast agent (indicated by a white arrow) is clearly enhanced compared to the control gland that did not receive an injection.

Figure 2 is a typical 3D volume-rendered T1W image showing the contrast-enhanced anatomy of mouse mammary ducts (orange circles) and lower aorta (red rectangles) for (a) an FVB/N mouse and (b) an SV40 mouse. Despite the relatively small luminal volume, the mammary ducts of both types of mice were easily detectable following an intra-ductal injection of a 0.8 mM solution of Omniscan. The FVB/N mouse and SV40 mouse have different ductal tree structures, and the FVB/N mouse has a much larger enhanced ductal volume at 12 – 21 minutes after injection than the SV40 mouse.

On average, the total volume of mammary gland with significant enhancement (Fig. 3(a)) in the first post-injection scan was about five times higher in FVB/N mice relative to SV40 mice ($p < 0.005$). Since the FVB/N mice on average weighed about 5 g more than the SV40 mice, the 'specific volume of enhancement' was also calculated by dividing the total volume of enhancement by the mouse weight. Figure 3(b) shows on average that the specific volume of enhancement was about four times higher ($p < 0.007$) in FVB/N mice relative to SV40 mice.

After the contrast agent was injected through the nipple and into the ducts, the contrast agent diffused into blood vessels from the mammary ducts, and was distributed to the rest of the body. Figure 4 shows box plots of the average contrast agent washout rate in (a) the mammary gland and (b) in the lower aorta for both FVB/N and SV40 mice. The average washout rate in the mammary gland was about 20% faster in SV40 mice ($p < 0.05$) relative to the FVB/N mice. The average rate of washout from the aorta was slower in the SV40 mice than in the FVB/N mice, but the difference was not statistically significant ($p = 0.16$).

4. Discussion

These results show that mammary ductal lumens with *in situ* cancer in SV40 mice are more permeable than normal ducts in FVB/N mice. The volume of the mammary glands with enhanced signal after the intra-ductal injection of contrast agent was five times higher in normal (FVB/N) glands than in SV40 glands with *in situ* cancer. This was not caused by

differences in the amount of contrast agent injected, since all mice received the same concentration and volume. The 'enhanced volume' was calculated relative to the signal intensity in the contralateral gland that did not receive an intra-ductal injection, to correct for any variations in signal between mice. The much smaller enhanced volume imaged between 12 minutes and 21 minutes after intra-ductal injection in SV40 mice could reflect rapid leakage of contrast agent from the SV40 ducts before acquisition of the first image, due to increased permeability of the ductal wall. In addition, the washout of the contrast agent from mammary ducts during the imaging period (from 12 minutes to 90 minutes post injection) is significantly more rapid in SV40 mice than in FVB/N mice, consistent with increased permeability of the walls of the ductal lumens.

After intraductal injection, contrast agent leaked out of mammary glands, diffused into the blood, and was cleared through renal excretion. Contrast agent washout rate measured from the aorta was somewhat slower in SV40 mice than in FVB/N mice (although this difference was not statistically significant). The slower decrease in washout rate of contrast agent in the aorta of SV40 mice suggests that the leakage rate from the ducts almost balances the rate of renal excretion, while in FVB/N mice, leakage from ducts is slower than renal excretion.

The present results are consistent with previous XFM (X-Ray Fluorescence Microscopy) data showing increased ductal permeability in the SV40 mice with *in situ* cancer [17]. XFM demonstrated that, following IV injection, Gadolinium that is taken up by mammary glands leaks into mammary ductal lumens in SV40 mice with *in situ* cancer, but there is no measurable leakage into the cancer-free ductal lumens of FVB/N mice. The XFM data provide further support for the hypothesis that increased permeability of mammary ducts of SV40 mice is due to the presence of small *in situ* cancers, and may be an MRI detectable marker for early cancer. This would be consistent with previous work showing increased permeability of epithelial tight junctions in mammary glands associated with *in situ* cancer [18].

The present results demonstrate that enhancement in the ductal lumens due to intra-ductal injection of a 0.8 mM solution of Omniscan is easily detectable and remains detectable for as long as 90 minutes. This is approximately the same as the concentration of contrast agent detected by XFM in SV40 mammary ducts following IV injection [17]. Therefore, the present results, together with previous XFM results suggest that contrast agent accumulation in hyper-permeable mammary/breast ducts following I.V. injection could be detected by MRI. Dynamic contrast enhanced (DCE) MRI is very sensitive and specific for invasive breast cancer but sensitivity and specificity for DCIS are more modest [4]. MRI is less sensitive to DCIS because intraductal cancer produces less angiogenesis than invasive cancer and DCIS is often diffuse. Therefore, there is a critical need for improved MRI-detectable markers for DCIS. DCE-MRI acquisition and analysis methods could be developed and used clinically for monitoring contrast media concentration in the ductal lumens following I.V. injection, as an early indicator of cancer. In addition, serial MRI studies of increasing ductal permeability in mouse models during cancer development, and changes in ductal permeability during therapy could guide the development of new therapies for human breast cancer and could enhance understanding of the biology of *in situ* breast cancers.

There were two major limitations in this study. First, the initial MRI scan was acquired approximately 12 min after the intra-ductal injection. Ideally, the initial MRI scan would start immediately after the intra-ductal injection to allow for a more accurate measurement of washout rates. This is currently difficult to do because of the time required to prepare the mouse for MRI after intra-ductal injection. However, we are currently developing methods that will decrease the time between an intra-ductal injection and the first MRI scan. In addition, we are performing measurements of ductal permeability using optical imaging methods, since optical scans can be acquired very rapidly after ductal injection. Second, the mammary glands of the SV40 mice studied in this research contained early *in situ* cancers and a small number of invasive tumors. More advanced cancers increase the difficulty of intra-ductal injection by blocking the flow of contrast agent throughout the ducts. To address this problem, we will develop gentler and more gradual injection protocols that allow us to measure permeability in the presence of *in situ* cancers at different stages and to more accurately assess changes in permeability as cancer develops.

Cancers in the SV40 mice start very early, as early as 4 weeks, and it would be important to collect information about the initiation of DCIS at this stage. It is currently difficult to perform an intra-ductal injection earlier than 15 weeks because the nipple is very small. We hope in the future to be able to develop better injection methods so that we can perform ductography on younger mice. However, even at 15 weeks we are able to study a range of cancers, because each mammary duct typically contains *in situ* cancers at different stages.

To our knowledge, this is the first dynamic 3D MRI study of contrast agent washout following intra-ductal injection into a mammary gland. The results of this pilot study provide support for the clinical use of ductography to find early cancers that are not detectable by traditional MRI. In addition, acquisition and analysis of DCE-MRI data after conventional I.V. injection of contrast media could be adapted to detect accumulation of contrast media in ductal lumens. MRI detection of increased ductal permeability could contribute to the clinical diagnosis of early *in situ* cancer, and changes in ductal permeability could be tracked as an indicator of response to therapy.

Acknowledgments

References

1. Bartlett JM, Nofech-Moses S, Rakovitch E. Ductal carcinoma in situ of the breast: can biomarkers improve current management? Clin Chem. 2014; 60:60–7. [PubMed: 24262106]

2. Esserman L, Alvarado M. Setting a research agenda for ductal carcinoma in situ that meets the current need for change. Ann Intern Med. 2014; 160:511–2. [PubMed: 24566896]

3. Nelson HD, O'Meara ES, Kerlikowske K, Balch S, Miglioretti D. Factors Associated With Rates of False-Positive and False-Negative Results From Digital Mammography Screening: An Analysis of Registry Data. Ann Intern Med. 2016; 164:226–35. [PubMed: 26756902]

4. Aminololama-Shakeri S, Flowers CI, McLaren CE, Wisner DJ, de Guzman J, Campbell JE, et al. Can Radiologists Predict the Presence of Ductal Carcinoma In Situ and Invasive Breast Cancer? AJR Am J Roentgenol. 2017:1–7.

5. Nicholson BT, Harvey JA, Patrie JT, Mugler JP 3rd. 3D-MR Ductography and Contrast-Enhanced MR Mammography in Patients with Suspicious Nipple Discharge; a Feasibility Study. Breast J. 2015; 21:352–62. [PubMed: 25882883]

6. Stearns V, Mori T, Jacobs LK, Khouri NF, Gabrielson E, Yoshida T, et al. Preclinical and clinical evaluation of intraductally administered agents in early breast cancer. Sci Transl Med. 2011; 3:106ra8.

7. Ishikawa T, Momiyama N, Hamaguchi Y, Takeuchi M, Iwasawa T, Yoshida T, et al. Evaluation of dynamic studies of MR mammography for the diagnosis of intraductal lesions with nipple discharge. Breast Cancer. 2004; 11:288–94. [PubMed: 15550848]

8. Slawson SH, Johnson BA. Ductography: how to and what if? Radiographics. 2001; 21:133–50. [PubMed: 11158649]

9. Behbod F, Kittrell FS, LaMarca H, Edwards D, Kerbawy S, Heestand JC, et al. An intraductal human-in-mouse transplantation model mimics the subtypes of ductal carcinoma in situ. Breast Cancer Res. 2009; 11:R66. [PubMed: 19735549]

10. Krause S, Brock A, Ingber DE. Intraductal injection for localized drug delivery to the mouse mammary gland. J Vis Exp. 2013

11. Markiewicz E, Fan X, Mustafi D, Zamora M, Roman BB, Jansen SA, et al. High resolution 3D MRI of mouse mammary glands with intra-ductal injection of contrast media. Magn Reson Imaging. 2015; 33:161–5. [PubMed: 25179139]

12. Green JE, Shibata MA, Yoshidome K, Liu ML, Jorcyk C, Anver MR, et al. The C3(1)/SV40 T-antigen transgenic mouse model of mammary cancer: ductal epithelial cell targeting with multistage progression to carcinoma. Oncogene. 2000; 19:1020–7. [PubMed: 10713685]

13. Jansen SA, Conzen SD, Fan X, Krausz T, Zamora M, Foxley S, et al. Detection of in situ mammary cancer in a transgenic mouse model: in vitro and in vivo MRI studies demonstrate histopathologic correlation. Phys Med Biol. 2008; 53:5481–93. [PubMed: 18780960]

14. Maroulakou IG, Anver M, Garrett L, Green JE. Prostate and mammary adenocarcinoma in transgenic mice carrying a rat C3(1) simian virus 40 large tumor antigen fusion gene. Proc Natl Acad Sci U S A. 1994; 91:11236–40. [PubMed: 7972041]

15. Fan X, Mustafi D, Markiewicz E, Zamora M, Vosicky J, Leinroth A, et al. Mammary cancer initiation and progression studied with magnetic resonance imaging. Breast Cancer Res. 2014; 16:495. [PubMed: 25510596]

16. Mustafi D, Zamora M, Fan X, Markiewicz E, Mueller J, Conzen SD, et al. MRI accurately identifies early murine mammary cancers and reliably differentiates between in situ and invasive cancer: correlation of MRI with histology. NMR Biomed. 2015; 28:1078–86. [PubMed: 26152557]

17. Jansen SA, Paunesku T, Fan X, Woloschak GE, Vogt S, Conzen SD, et al. Ductal carcinoma in situ: X-ray fluorescence microscopy and dynamic contrast-enhanced MR imaging reveals gadolinium uptake within neoplastic mammary ducts in a murine model. Radiology. 2009; 253:399–406. [PubMed: 19864527]

18. Kominsky SL, Argani P, Korz D, Evron E, Raman V, Garrett E, et al. Loss of the tight junction protein claudin-7 correlates with histological grade in both ductal carcinoma in situ and invasive ductal carcinoma of the breast. Oncogene. 2003; 22:2021–33. [PubMed: 12673207]
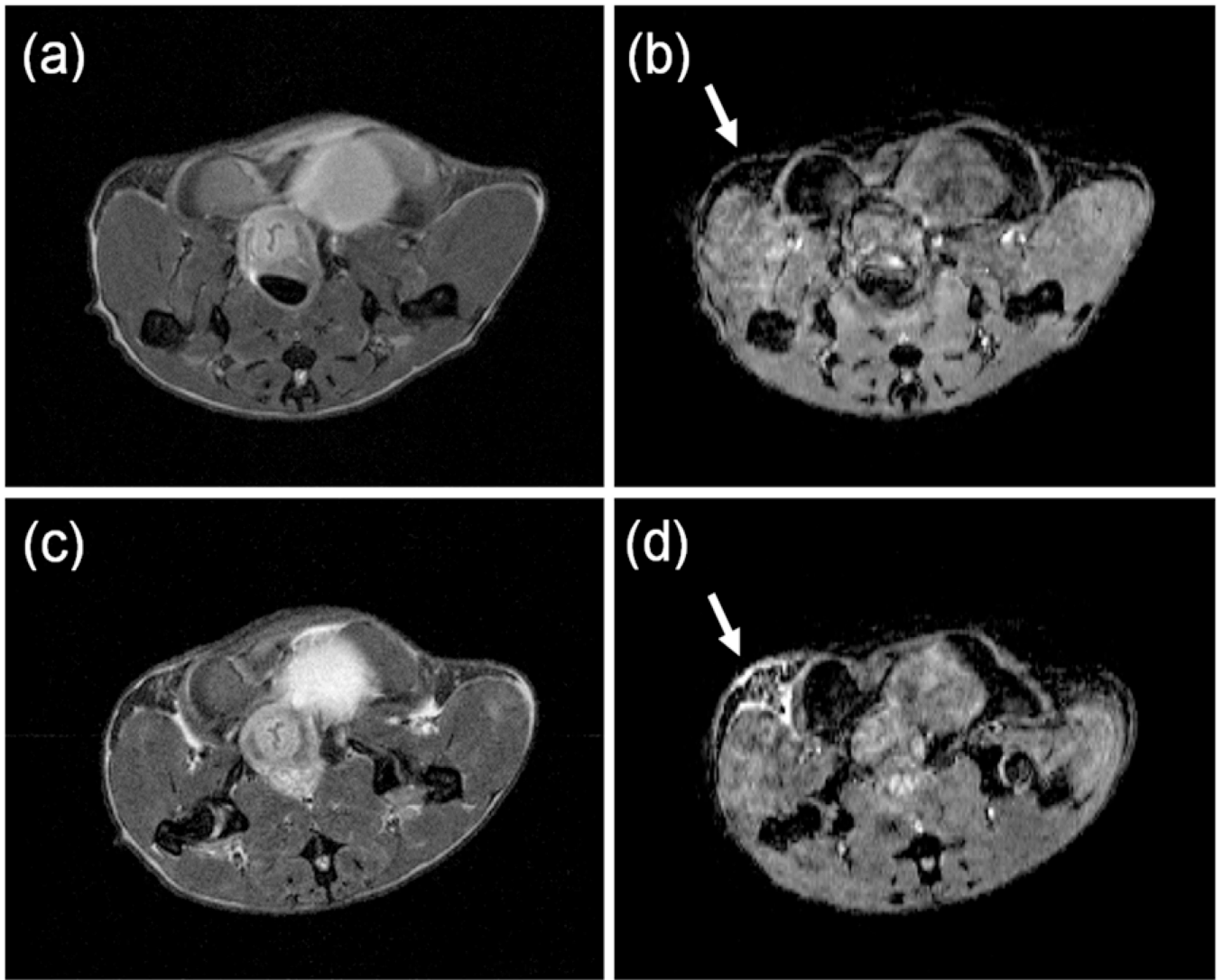
Figure 1.
An axial MRI slice for an SV40 mouse: (a) pre-contrast agent injection T2-weighted image, (b) a corresponding pre-contrast agent injection T1-weighted image, (c) ~90 min post-contrast agent injection T2-weighted, and (d) the corresponding 1st T1-weighted image post-contrast agent injection. The side of mammary gland injected with contrast agent is indicated by a white arrow and the bright area indicates contrast agent uptake.
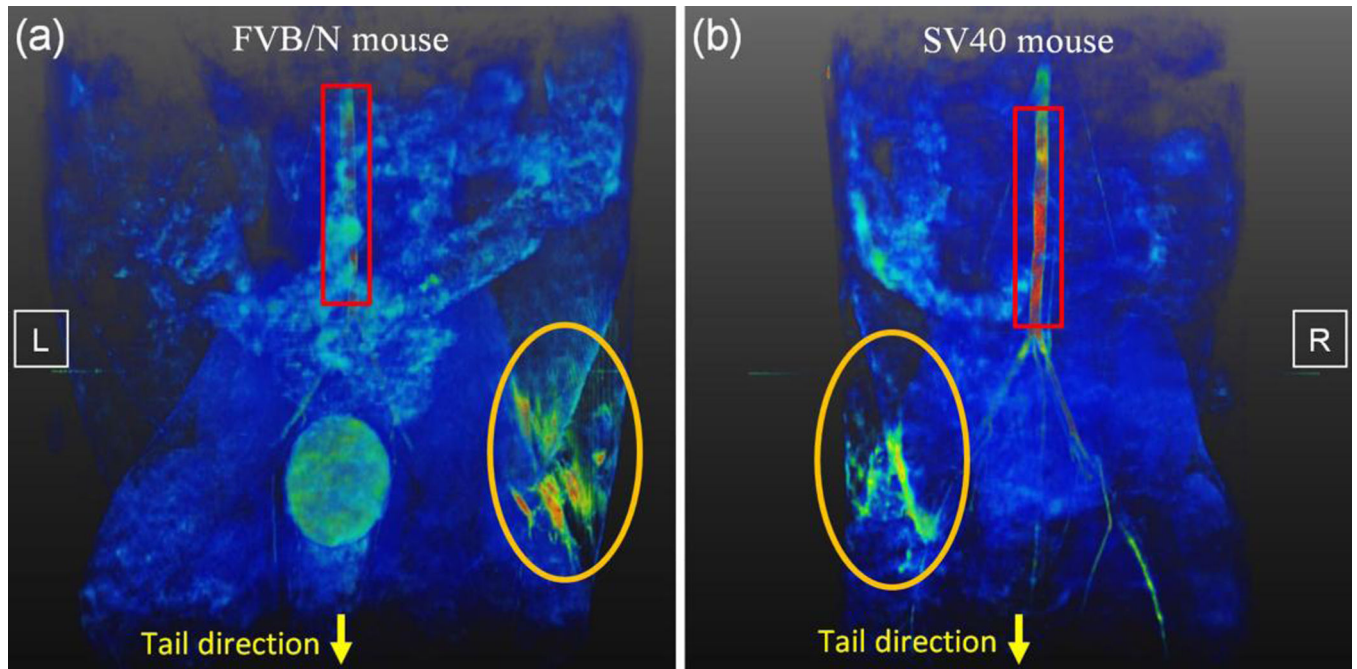
Figure 2.
Volume rendered T1-weighted images were generated to show contrast agent uptake by a mouse inguinal mammary gland (orange circles) and lower aorta (red rectangles) for (a) an FVB/N mouse and (b) a SV40 mouse on one side of inguinal gland. Please note that part of aorta for FVB/N mouse was hidden behind other tissues. The image shows the body orientation where the tail is located at the bottom of the image. The left (L) and right (R) side were labeled on the figures.
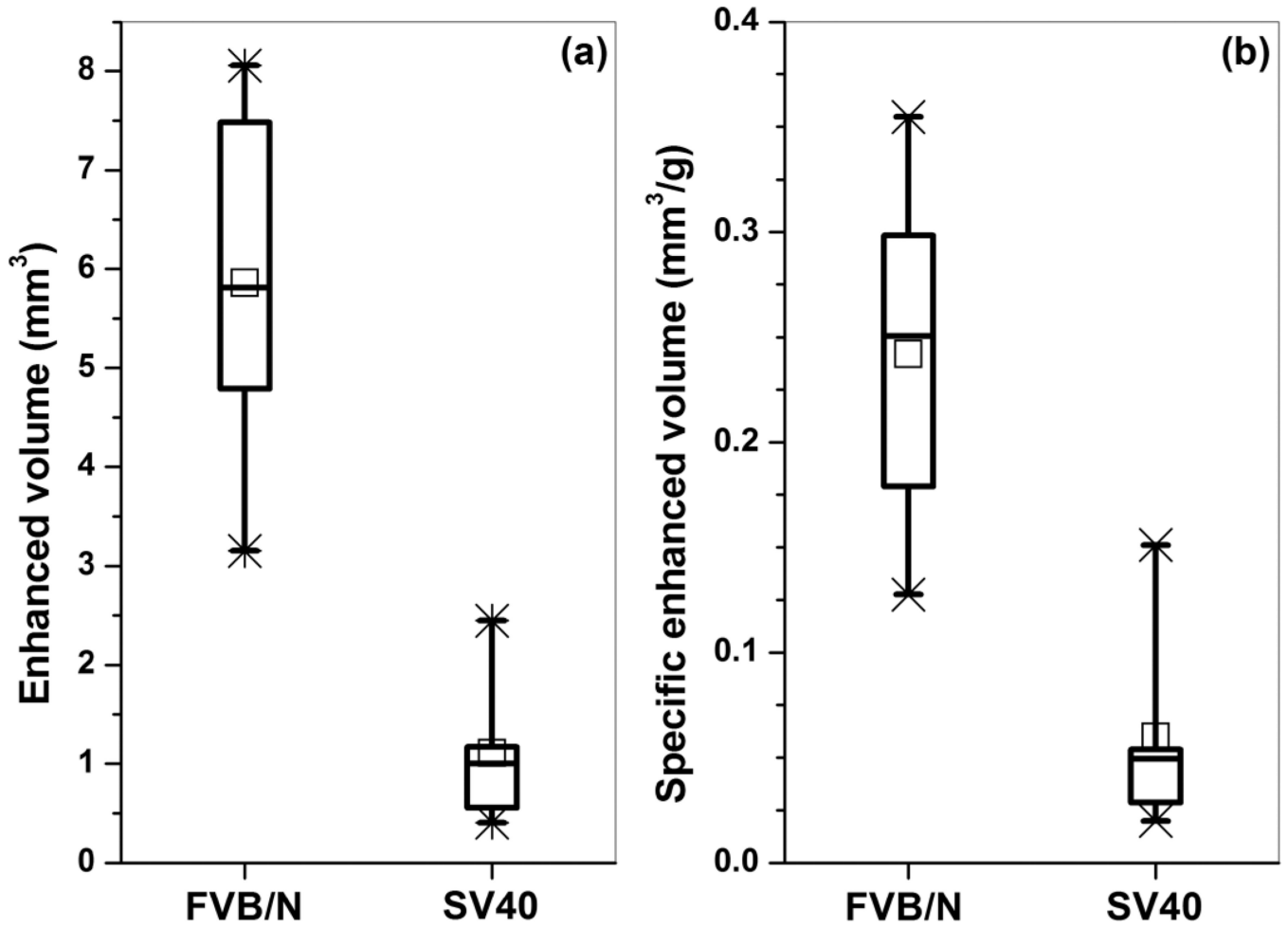
Figure 3.
Box plot of (a) total volume of tissue and (b) specific volume of tissue that had significant enhancement post contrast agent injection for an FVB/N mouse and an SV40 mouse after one side of an inguinal gland was injected with contrast agent. The square symbols (□) indicate the mean, and the asterisks (*) indicate the upper and lower limits of the data.
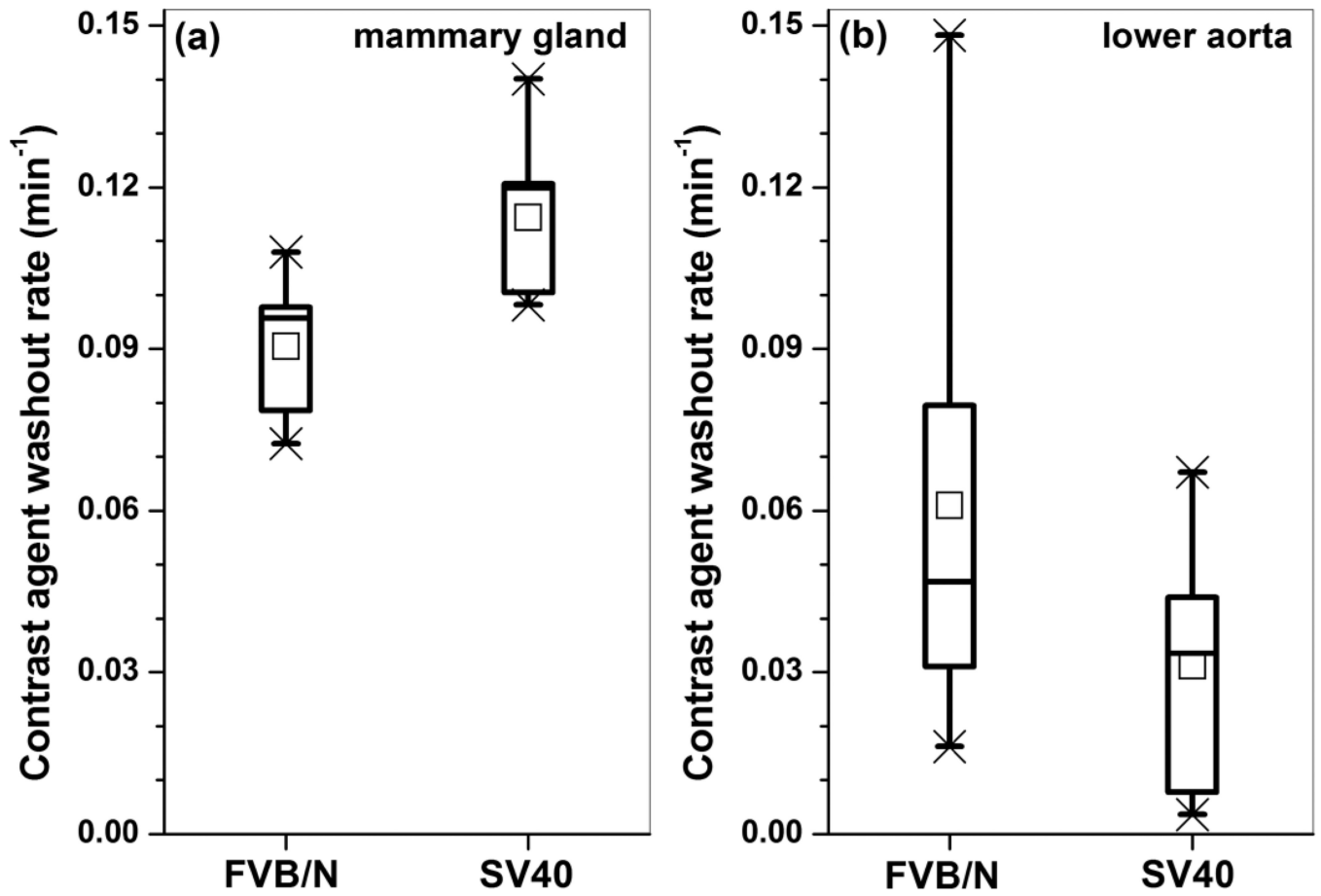
Figure 4.
Box plots of average contrast agent washout rate for tissue that had significant contrast uptake in (a) mammary gland and (b) lower aorta for both FVB/N and SV40 mice. The square symbols (□) indicate the mean, and the asterisks (*) indicate the upper and lower limits of the data.

Table 1

Numbers of *in situ* cancers and small invasive tumors were found in eight (A – H) SV40 mice in the inguinal mammary glands by examining all MRI slices through the glands.

	A	B	C	D	E	F	G	H
in situ cancer	5	8	4	2	2	5	3	2
Invasive tumor	0	2	1	2	2	1	0	2